Journal of Physics:
Conference Series

PAPER • **OPEN ACCESS**

Updates of the atmospheric monitoring at the Pierre Auger Observatory

To cite this article: Max Büsken *et al* 2025 *J. Phys.: Conf. Ser.* **2985** 012001

Updates of the atmospheric monitoring at the Pierre Auger Observatory

Max Büsken[1,2], Bianca Keilhauer[3] for the Pierre Auger Collaboration[4]

[1]Karlsruhe Institute for Technology (KIT), Institute of Experimental Particle Physics, Karlsruhe, Germany

[2]Universidad Nacional de San Martín (UNSAM), Instituto de Tecnologías en Detección y Astropartículas, Buenos Aires, Argentina

[3]Karlsruhe Institute for Technology (KIT), Institute for Astroparticle Physics, Karlsruhe, Germany

[4]Observatorio Pierre Auger, Av. San Martín Norte 304, 5613 Malargüe, Argentina
Full author list: https://www.auger.org/archive/authors_2024_07.html

E-mail: spokespersons@auger.org

Abstract. Recent developments for the atmospheric monitoring at the Pierre Auger Observatory are presented. These developments include a new method for cloud identification based on night sky background data from the Fluorescence Detector, a new network of devices for measuring the electric field across the array of the observatory, and updates of lidar data applied to identify clouds for high-level physics analyses of air shower data.

1 Introduction

At the Pierre Auger Observatory we detect air showers produced by ultra-high energy cosmic rays using several different detector types, such as the Water Cherenkov Detector (WCD), the Fluorescence Detector (FD), the Underground Muon Detector (UMD), and the Radio Detector (RD) [1, 2]. For a thorough interpretation of the extensive air showers, profound understanding and observation of atmospheric conditions at the Observatory are needed [3]. For this purpose, the Pierre Auger Collaboration has installed a quite comprehensive suit of instruments for atmospheric monitoring, cf. Fig. 4.

2 Night sky background data from the Fluorescence Detector

The Fluorescence Detector of the Pierre Auger Observatory is recording the night sky background (NSB) during the regular data acquisition of extensive air showers. For every pixel of the 20 x 22 PMTs cameras in every FD station, the photon flux from the background is measured and stored every 30 seconds [1]. As a substitute for the cloud cameras, we can use this huge amount of data to infer a threshold photon flux for every pixel of all cameras and for every sidereal time which represents clear visibility in the field of view. After having determined this photon flux for clear conditions, the variations of the NSB data indicate the presence of clouds in the field of view of the telescopes. Pixels with photon flux values larger than this threshold are classified as clear, while those falling below are categorised as cloudy.

This method has been firstly developed for the FD station Coihueco + HEAT (High-Elevation Auger Telescopes). For a given time, the photon fluxes of all pixels are plotted, grouped by their elevation [4].

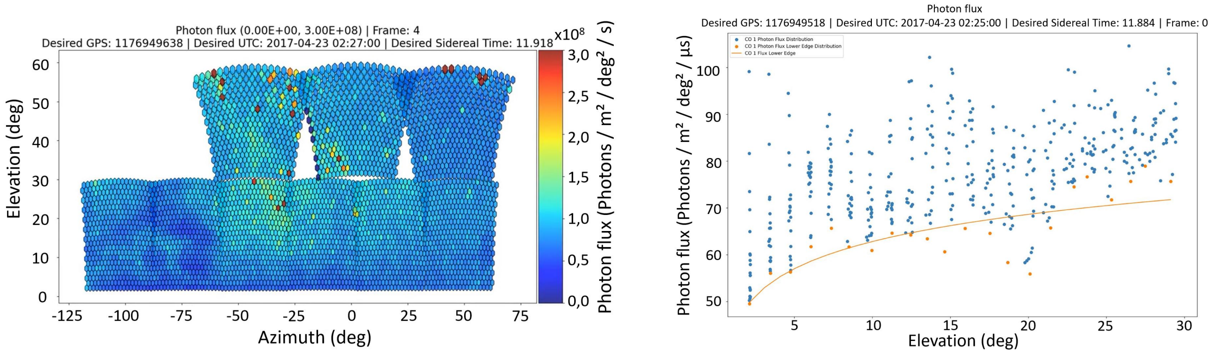

Figure 1: Left: Example of a NSB record of the FD station Coihueco + HEAT with six telescopes plus three elevated telescopes, each consisting of 20 x 22 PMTs. Right: NSB flux vs. elevation of one telescope. Blue points represent the photon flux for each pixel plotted by elevation. Orange points represent minimum photon flux-elevation pairs and the photon flux lower edge plotted as logarithmic fit (orange line) to set of orange points.

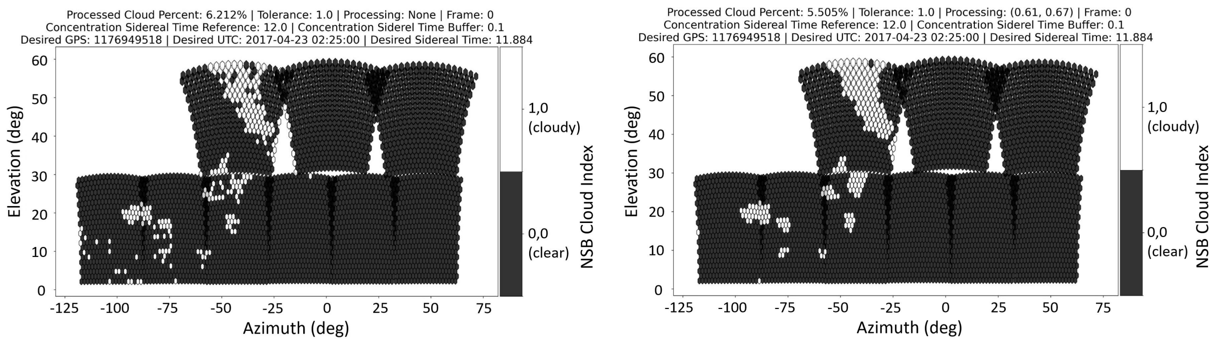

Figure 2: Example of a cloud representation for the FD station Coihueco + HEAT. Left: Without smoothing algorithm. Right: With applied smoothing algorithm.

The minimum flux of each elevation is then fitted by a logarithmic curve, see Fig. 1, right. After deriving the logarithmic curves for a given telescope and sidereal time for a full year, concentration diagrams of those flux curves can be plotted from which the clear-sky threshold as a function of elevation, for each telescope at each sidereal time can be derived. Based on this threshold for every pixel of a telescope, the classification between clear and cloudy in the field of view of every pixel can be performed reading out the actual NSB photon flux. Introducing a tolerance factor for the pixel classification allows to adjust the sensitivity of the cloud detection.

Finally, a smoothing algorithm is applied to the cloud image processing to compensate for e.g. noisy pixels of the telescope. The algorithm considers the information from surrounding pixels, so that the derived images of clouds are properly displayed at the telescopes' field of view. An example of a cloud representation for the FD station Coihueco + HEAT is shown in Fig. 2 where in the left part the cloud classification is shown without smoothing algorithm and in the right part with applying it.

The newly derived cloud representation for every pixels is validated by the cloud information from infrared (IR) cloud cameras which were operated at the Auger Observatory for many years at every FD station. IR cloud camera data have been provided for every 5 minutes (15 minutes for HEAT) during data taking with the fluorescence detector and the cloud classification was given in six bins between clear (0) and cloudy (5). For comparing with the binary information of the new method, IR cloud indices between 0 and 2 are summarized as clear while indices of 3 and higher represent cloudy conditions. Using the clear-sky thresholds derived with the new method from 2017 data and apply them to periods during 2018, it can be stated that the procedure shows already quite good results, even though more detailed improvements on several stages of the procedure are needed. For example during periods with partial cloud coverage, the agreement between old IR cloud information and new NSB cloud information is

Figure 3: One of the new EFM stations, close to the Loma Amarilla FD site.

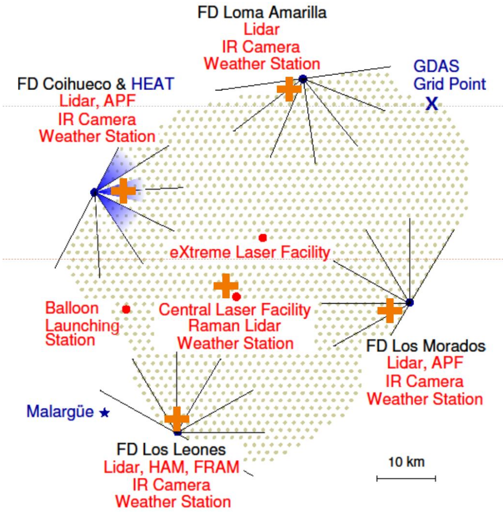

Figure 4: Schematic map of the installations for atmospheric monitoring. The orange crosses indicate the positions of the electric field mills.

more scattered. Next steps for consolidating the new procedure include improvements for the clear-sky threshold determination, evaluating the tolerance factor, and the determination of the threshold for all FD telescopes and relevant sidereal times. Then the newly derived cloud information can be applied to further periods and telescopes to compare it with the IR cameras data. After this consolidation, the new method can be applied for filling up cloud information during all periods without IR camera records.

3 New setup for E-field measurements

A major part of the AugerPrime upgrade of the Pierre Auger Observatory is the installation of the Radio Detector (RD) [5]. Radio detection of air showers was successfully engineered at the Observatory with the Auger Engineering Radio Array (AERA), consisting of 153 antenna stations across an area of about 17 km^2. The RD is designed with the knowledge gained from deploying and operating AERA and aims at detecting inclined air showers at the highest energies. At the largest inclinations, the radio signal distributions at ground, often called *footprints*, become wide stretched ellipses with lengths up to several tens of km. The RD will consist of 1660 antenna stations, each on top of every surface detector station, across the full observatory area of more than 3000 km^2 and its deployment is expected to be complete by the end of 2024. As of end of July 2024, 952 antennas are already in the field.

Air-shower radio emission is nowadays well understood and the radio-detection technique is competing with established methods (see [6] and [7] for reviews). Usually, most of the radio emission is generated from charged particles of the shower being deflected in the geomagnetic field. However, large atmospheric electric fields can alter the radio emission and completely change the electric field polarization of the radio signals [8, 9]. Therefore, air showers detected during thunderstorms with large atmospheric electric fields need to be vetoed, requiring permanent monitoring of the atmospheric electricity.

At the Pierre Auger Observatory, two electric field mills[1] (EFMs) are deployed at AERA that measure the electric field at a sampling rate of 1 Hz. In cosmic-ray analyses with AERA, candidate events are usually rejected if one of either station measured electric fields exceeding a defined limit for at least a few minutes around the time of the event. The antenna array of the RD has a significantly larger area and the development of inclined showers, which is where electric fields would affect the radio emission, can happen far away from the core of the signal footprint at ground. Therefore, electric field monitoring on a large scale is required. A network of five new EFMs at the Auger Observatory of the same type as those used at AERA have been installed. One of the new stations is depicted in Fig. 3. They were deployed in August and November 2022 and their technical setup was described in [10]. By design of the stations, the E-field measurements have an absolute calibration with an accuracy estimated at 6.5% [11, 12]. Four

[1]Campbell Scientific CS110 Electric Field Meter

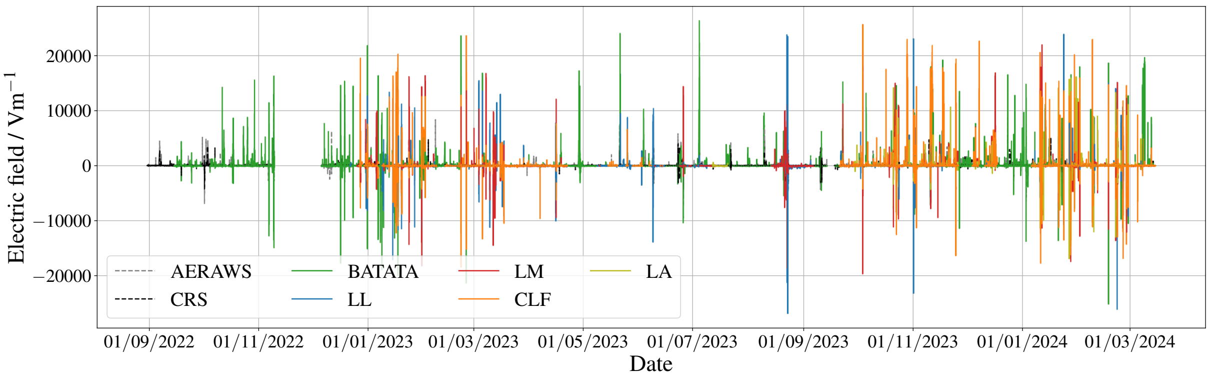

Figure 5: All E-field recordings from the deployment of the new stations until mid March 2024. AERAWS and CRS are the two E-field mills at AERA. The newly deployed stations with absolute calibration are BATATA, LL, LM, CLF and LA.

of the five stations are located within a few km distance to each of the four FD buildings, close to the border of the array. The fifth station is installed at the CLF in a central position, see Fig. 4.

The data collected from the deployment of the new stations until mid March 2024 are shown in Fig. 5. While E-field strengths are within the fair-weather regime for most of the time, strengths of a few tens of kV/m are observed during thunderstorms. The rate of thunderstorms is larger during austral summer compared to winter.

Individual thunderstorms are seen to come in different sizes and yielding different E-field traces. Some thunderstorms appear to be smaller sized, only being detected in one station at a time with similarly shaped E-field traces recorded in two stations separated in time. Those thunderstorms may be traceable in their movement across the array. Air showers that were detected by the RD and that developed in the region of the backtraced thunderstorm may have produced radio signals altered by the E-field and can thus be rejected. Showers that developed in other parts of the array, where no large E-fields were recorded, can safely be used in analyses.

In other cases, large E-fields were measured in all stations simultaneously for periods of hours, indicating large-sized thunderstorm activity across the entire observatory. Those periods must likely be rejected overall for air-shower analyses.

Aside from the application to the RD, the E-field data recorded by the new stations could be useful to cosmo-geophysics-related research. One potential aspect that could benefit from the E-field information are studies of terrestrial gamma-ray flashes [13]. Transregional and global studies of atmospheric electricity, e.g. related to the global electric circuit, make use of data from multiple E-field sensors around the world [14, 15]. The new E-field mill network at the Observatory could also make a significant contribution to this kind of research.

4 Update of lidar data

In its original design, a lidar facility was operated at each of the four FD stations at the Auger Observatory. However several hardware failures and further constraints led to the current situation of two lidar stations being operational, at the FD stations Coihueco and Loma Amarilla.

The lidars at the Auger Observatory follow three scan procedures, of which two are close to, but outside the field of view of the FD, and one short scan is performed every hour in the FD field of view vetoing the regular FD data taking. From these lidar scans, cloud information is derived per hour, providing the cloud coverage, the cloud base height, and the cloud optical depth [16]. On average, about 70% - 80% of the times of FD data taking are covered by lidar information, if the lidar station is operational. From these lidar records we find that for the Auger Observatory the cloud coverage is below 10% for 43% to 53% of the periods with lidar records for the different lidar sites. Only about 14% to 18% of the lidar records show cloud coverage between 10% and 90%. Periods with cloud coverage of more than 90% are recorded for 29% up to 43% of the time. Furthermore, it can be assumed that about half of the missing lidar data, during general operational phases, are due to interrupted lidar scans because of bad weather. Then periods with low cloud coverage almost equal to periods with highest cloud coverage.

For cloudy periods, the lidar records indicate a minimum cloud base height of about 2 to 3 km above

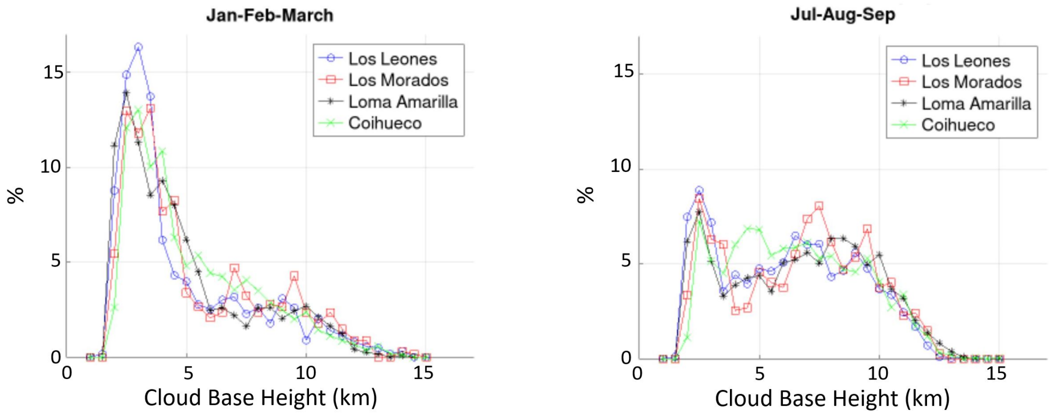

Figure 6: Distribution of minimum cloud base heights from lidar scans at the four FD stations, grouped by trimesters. Left: January to March. Right: July to September.

the array between about 10% and 15% of the time. The shape of the distribution of the cloud base heights can be grouped by trimesters. While for January to March, the minimum cloud base height is clearly peaked at about 2 to 3 km in its appearance, the distribution is rather broad during July to September with cloud base heights between about 2 to 10 km above the array, see Fig. 6. The other two trimesters show a kind of transition where the low height peak is less pronounced but visible and a second pronounced, but broad distribution of cloud base heights between about 5 to 10 km appears.

Based on this recent lidar data analysis, the atmospheric homogeneity with respect to clouds across the Auger Observatory is evaluated. For this, coincident periods between two respective sites are compared in terms of cloud coverage and cloud base height. For cloud coverage below 10%, we find coincidences between 34% to 44% of the time between two respective sites with highest coincidence between the closest two sites Coihueco and Loma Amarilla, as expected. For high cloud coverage of more than 90%, the coincidences vary between 19% and 28%. For these conditions, Coihueco behaves in a special way because of downwind turbulance from the Andes. For the comparison based on minimum cloud height, we separate the conditions between base height below and above 5 km. For low cloud conditions, the coincidence rates are between 24% and 30% for two respective sites, while the coincidences are much higher for high cloud conditions with 55% to 59%. This leads to the overall conclusion that high clouds are typically seen by more than one FD site and low clouds are often local phenomena. Adding up these conditions of agreement, the pair Los Morados and Loma Amarilla is most homogeneous, while Los Morados and Coihueco is maximal inhomogeneous.

The updated lidar information is currently implemented into the full reconstruction chain for extensive air showers detected by the fluorescence detector. The lidar data are used together with cloud-camera data, GOES satellite data, and bistatic lidar (central laser facilities) data to discard cosmic-ray events when too many clouds are present in the FD field of view from high-level physics analyses of extensive air showers.

5 Summary and Outlook

In light of the AugerPrime upgrade of the Pierre Auger Observatory and data taking entering into a second phase lasting for another decade, we report on developments regarding the atmospheric monitoring at the Observatory. These developments provide better understanding of our air-shower calorimeter that is crucial for analyzing the cosmic ray events. A new method using night sky background data from the fluorescence detector enables permanent cloud coverage measurements at all times with good performance. This is especially helpful for data periods when cloud-coverage measurements from IR cameras are not available.

A new network of electric field mills across the observatory has been deployed and is running smoothly. This network permanently monitors the atmospheric electricity with the main task of providing a thunderstorm veto for radio measurements of air showers by the new radio detector since those measurements are significantly altered in the presence of large atmospheric electric fields.

Finally, an updated analysis of lidar data gives new insights into cloud characteristics at the observatory during air-shower measurements with the fluorescence detector. Studies of the cloud base heights exhibit a clear seasonal dependence. With an updated lidar database, the selection of air-shower events for physics analyses will be improved.

Acknowledgments

Part of this research was supported by the *Bundesministerium für Bildung und Forschung* (BMBF), grant no. 05A23VK4, and by the *Hermann von Helmholtz-Gemeinschaft Deutscher Forschungszentren e.V.* through the Helmholtz International Research School for Astroparticle Physics and Enabling Technologies (HIRSAP, grant no. HIRS-0009) of Initiative and Networking Fund.

References

[1] A. Aab *et al.*, Pierre Auger Collaboration, "The Pierre Auger Cosmic Ray Observatory," *Nucl. Instrum. Meth. A* **798** (2015) 172–213, arXiv:1502.01323 [astro-ph.IM].

[2] A. Abdul Halim *et al.*, Pierre Auger Collaboration, "Highlights from the Pierre Auger Observatory," *PoS* **ICRC2023** (2023) 016, arXiv:2312.14673 [astro-ph.HE].

[3] B. Keilhauer, "Atmospheric Monitoring for Astroparticle Physics Observatories," *PoS* **ICRC2023** (2024) 021.

[4] J. Ahumada-Becerra, "Cloud Detection Using Fluorescence Detectors at the Pierre Auger Observatory," M.Phil. thesis, University of Adelaide, Australia, 2024. https://hdl.handle.net/2440/141660.

[5] A. Abdul Halim *et al.*, "Status and expected performance of the AugerPrime Radio Detector," *PoS* **ICRC2023** (2023) 344.

[6] T. Huege, "Radio detection of cosmic ray air showers in the digital era," *Phys. Rep.* **620** (Mar., 2016) 1–52, arXiv:1601.07426 [astro-ph.IM].

[7] F. G. Schröder, "Radio detection of cosmic-ray air showers and high-energy neutrinos," *Progr. Part. Nucl. Phys.* **93** (2017) 1–68.

[8] S. Buitink *et al.*, "Amplified radio emission from cosmic ray air showers in thunderstorms," *Astron. Astrophys.* **467** no. 2, (May, 2007) 385–394, arXiv:astro-ph/0702432 [astro-ph].

[9] P. Schellart *et al.*, "Probing Atmospheric Electric Fields in Thunderstorms through Radio Emission from Cosmic-Ray-Induced Air Showers," *Phys. Rev. Lett.* **114** (Apr, 2015) 165001.

[10] M. Büsken *et al.*, "A new network of electric field mills at the Pierre Auger Observatory," *Journal of Physics: Conference Series* **2398** no. 1, (Dec, 2022) 012004.

[11] Campbell Scientific, Inc., "CS110 electric field meter product manual." https://s.campbellsci.com/documents/us/manuals/cs110.pdf. accessed 6-July-2021.

[12] A. Hinckley. Consultation with Campbell Scientific.

[13] J. Dwyer, A. Abdul Halim, *et al.*, "Study of downward Terrestrial Gamma-ray Flashes with the surface detector of the Pierre Auger Observatory," *PoS* **ICRC2023** (2023) 439.

[14] D. Siingh, R. Singh, N. J. Victor, and A. Kamra, "The DC and AC global electric circuits and climate," *Earth-Science Reviews* **244** (2023) 104542.

[15] J. Tacza, J.-P. Raulin, C. Morales, E. Macotela, A. Marun, and G. Fernandez, "Analysis of long-term potential gradient variations measured in the Argentinian Andes," *Atmospheric Research* **248** (2021) 105200.

[16] J. Rodriguez *et al.*, Pierre Auger Collaboration, "Measurements of Cloud Base Height and Coverage using Elastic Multiangle Lidar Scans at the Pierre Auger Observatory," *PoS* **ICRC2023** (2023) 374.